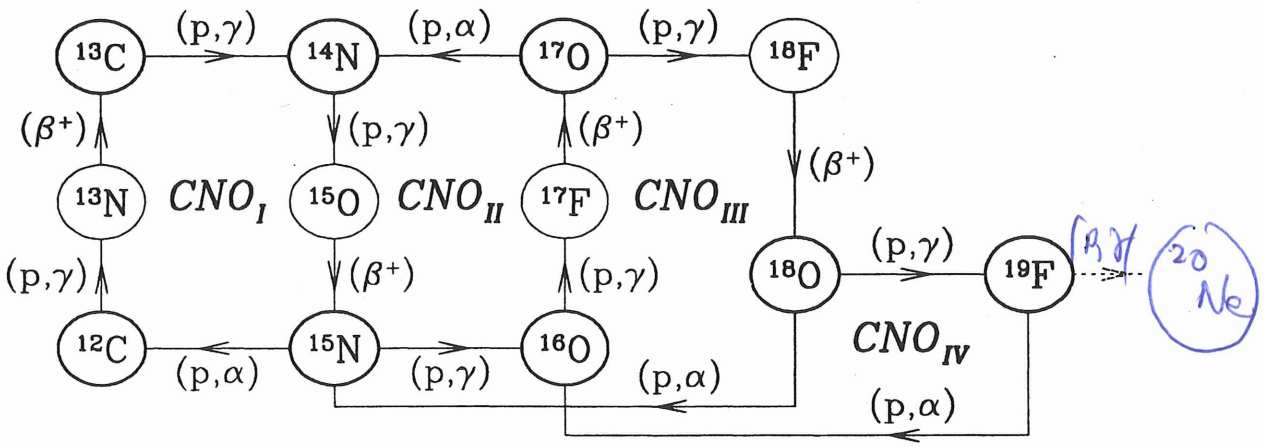

Figure 1: Reactions of the CNO cycles. Stable nuclides are enclosed in thick circles. The dashed line represents the possible leakage out of the cycles.

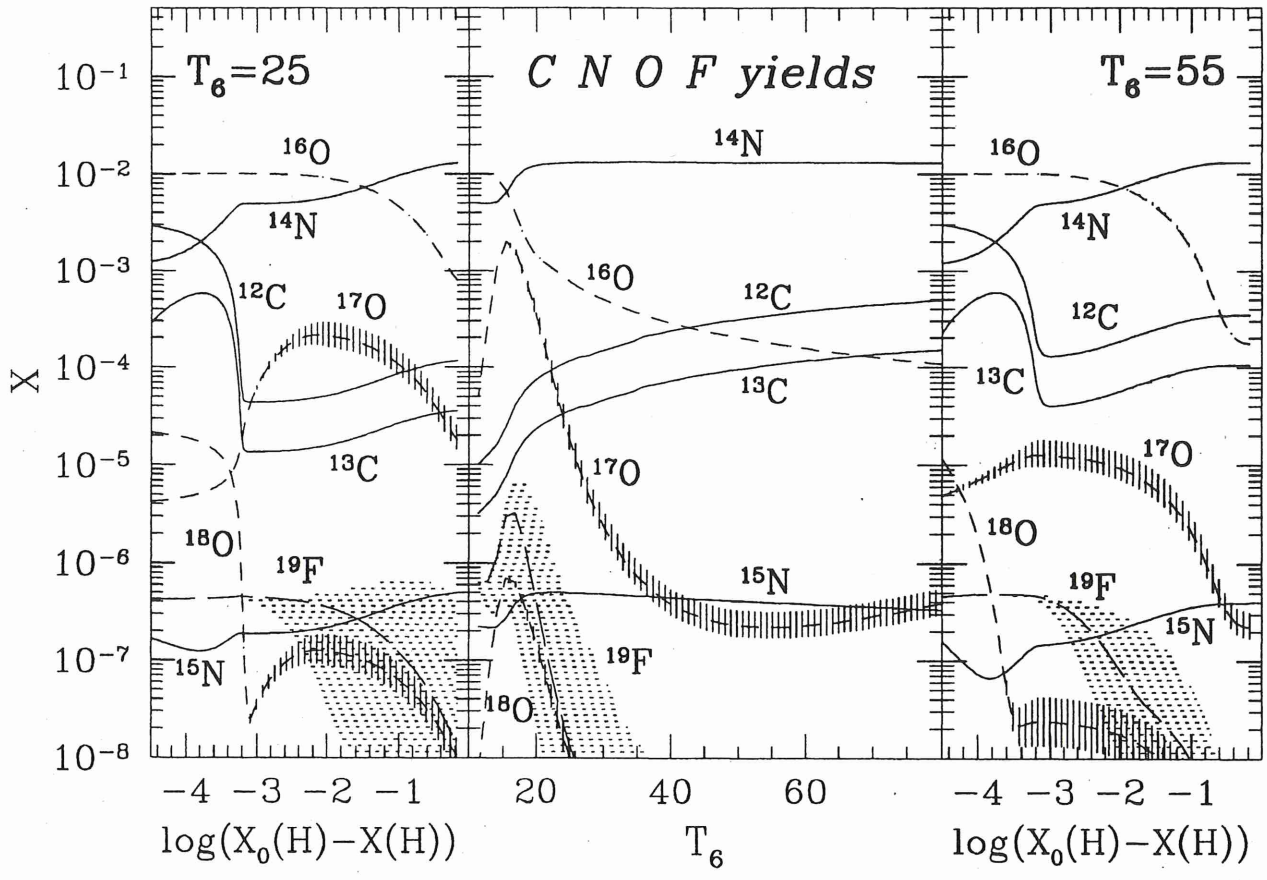

Figure 2: *Left and right panels:* Time evolution of the mass fractions of the stable nuclides involved in the CNO cycles versus the amount of hydrogen burned at constant temperatures $T_6 = 25$ and 55 and density $\rho = 100$ g/cm^3; *Middle panel:* Mass fractions of these nuclides at H exhaustion [X(H)=10^{-5}] versus T_6.

ARNOULD, MOWLAVI & CHAMPAGNE 1995, Liège conf.

H-BURNING CHAINS

- NeNa
- MgAl
- $\langle \sigma v \rangle$: some large uncertainties (Iliadis, §5.1.3)

NeNa

- Na enrichments in giants & supergiants : $^{22}Ne \rightarrow {}^{23}Na$

MgAl

- a source of ^{26}Al and $^{26}Al^m$

^{26}Al —97%→ $^{26}Mg + \gamma + 1.81\ MeV$

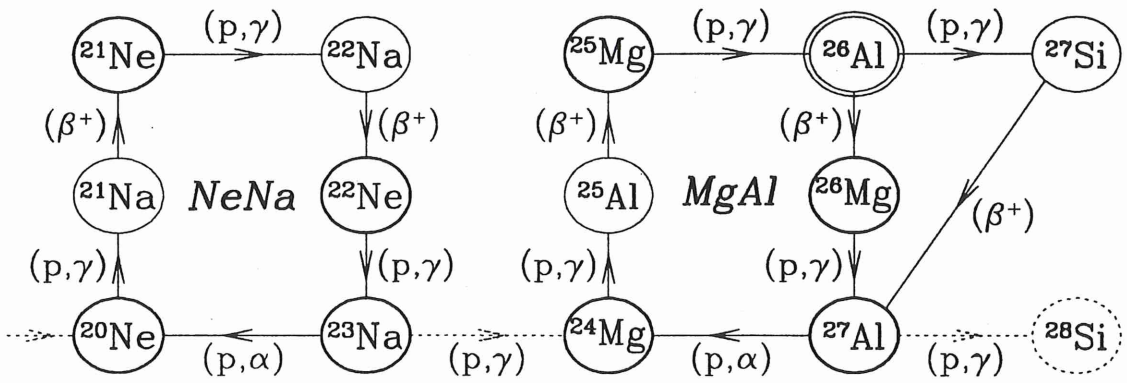

Figure 5: Same as Fig. 1, but for the NeNa and MgAl chains. The ground and isomeric states of ^{26}Al are considered as two separate species.

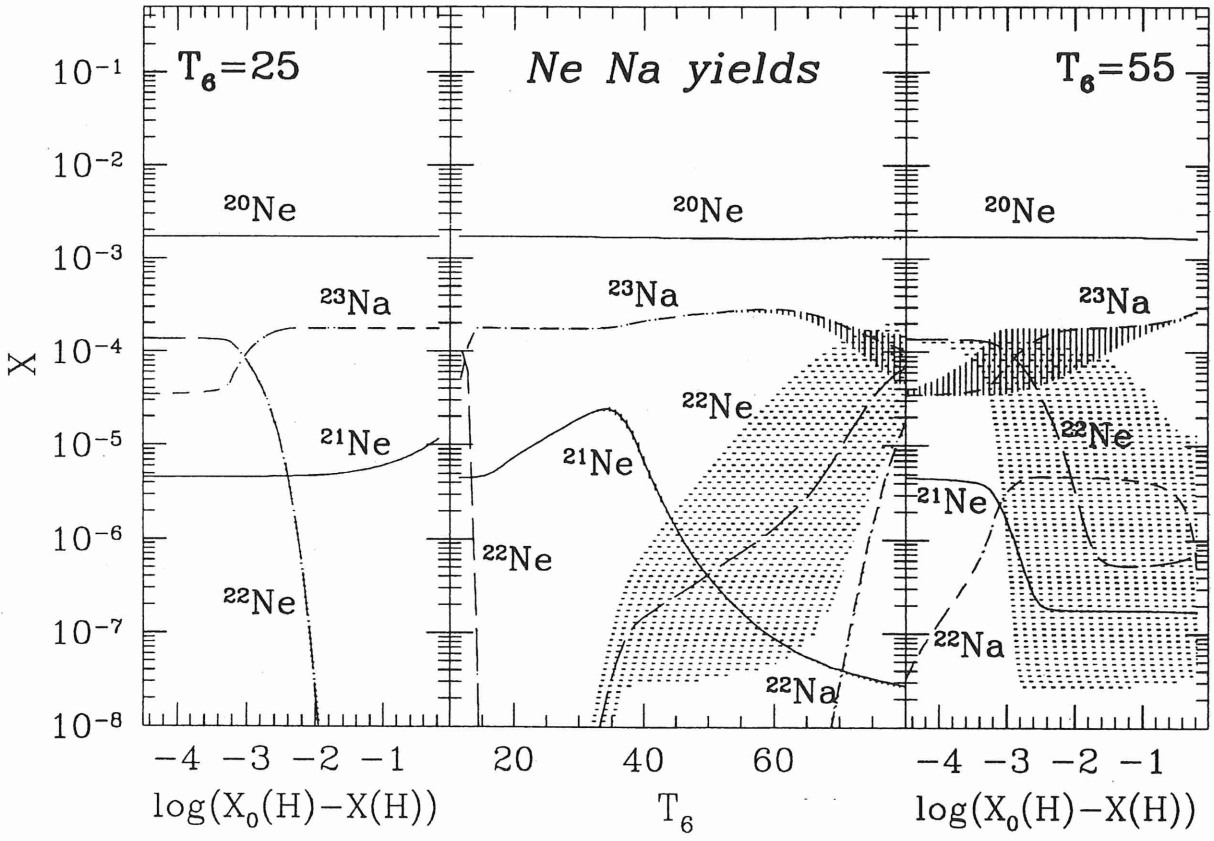

Figure 6: Same as Fig. 2, but for the nuclides involved in the NeNa chain.

^{21}Ne is destroyed by $^{21}\mathrm{Ne}(\mathrm{p},\gamma)^{22}\mathrm{Na}(\beta^+)^{22}\mathrm{Ne}$. As a result, the ^{21}Ne abundance at H exhaustion is maximum when the burning proceeds at a temperature in the approximate $30 \lesssim T_6 \lesssim 35$ range. This conclusion is not affected by the less than 40% uncertainty reported by El Eid and Champagne (1995) for $^{21}\mathrm{Ne}(\mathrm{p},\gamma)^{22}\mathrm{Na}$, and would even remain basically unaltered with the

$\beta^+ \longleftrightarrow$ p-capture

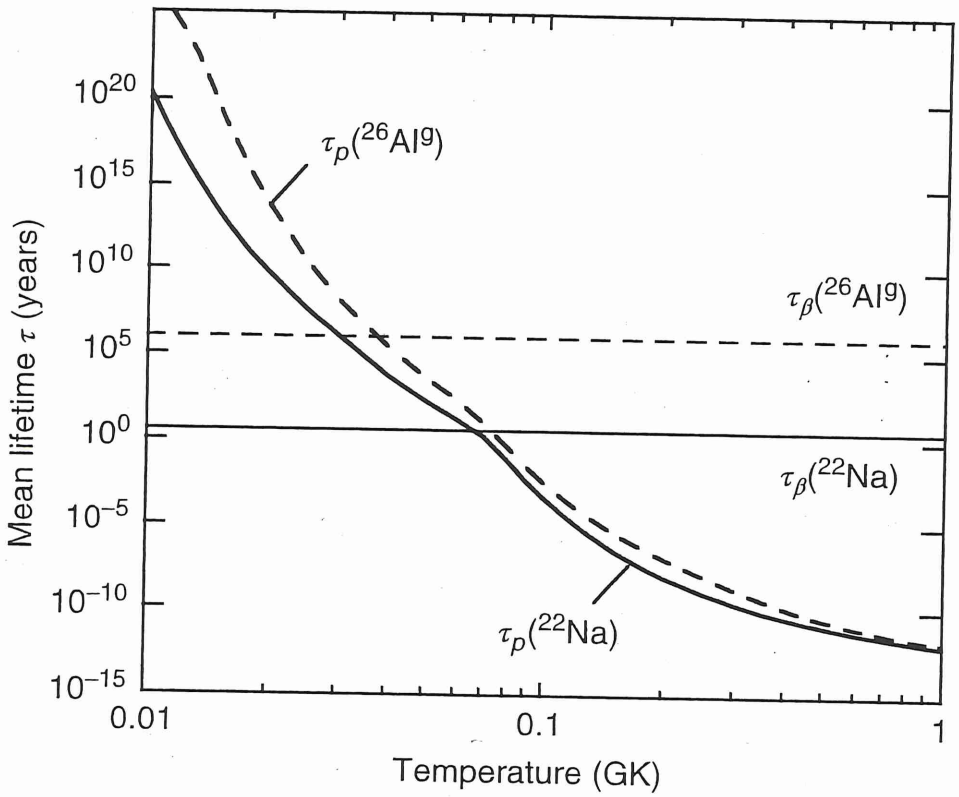

Figure 5.16 Mean lifetimes of ^{22}Na (solid lines) and ^{26}Al^g (dashed lines) versus temperature. The curves are calculated for the conditions $\rho = 100$ g/cm^3 and $X_H/M_H = 1$. The mean lifetimes for the β^+-decays, $\tau_\beta(^{22}\text{Na})$ and $\tau_\beta(^{26}\text{Al}^g)$, are independent of temperature and density for the conditions of hydrostatic hydrogen burning.

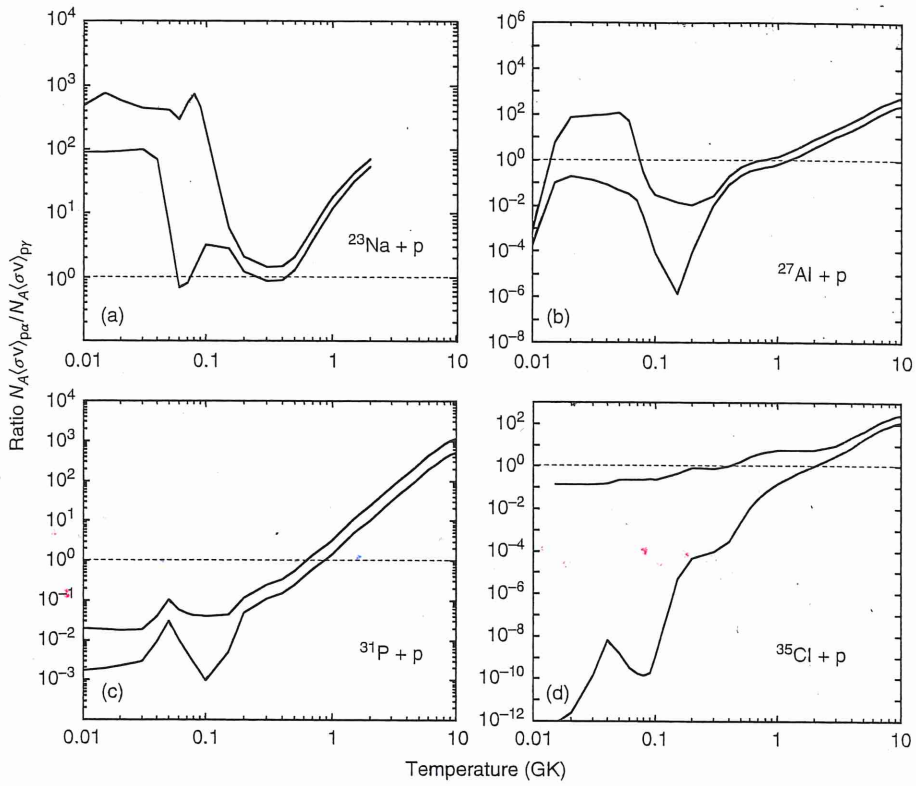

Figure 5.17 Branching ratio $B_{p\alpha/p\gamma} = N_A\langle\sigma v\rangle_{(p,\alpha)}/N_A\langle\sigma v\rangle_{(p,\gamma)}$ versus temperature for the reactions (a) ^{23}Na + p, (b) ^{27}Al + p, (c) ^{31}P + p, and (d) ^{35}Cl + p. The two solid lines in each panel represent the upper and lower boundaries of $B_{p\alpha/p\gamma}$. The area between the solid lines indicates the uncertainty in $B_{p\alpha/p\gamma}$ that is caused by unknown contributions to the (p,γ) and (p,α) reaction rates.

BRANCHING RATIOS (p,α)/(p,γ)

^{23}Na ^{27}Al

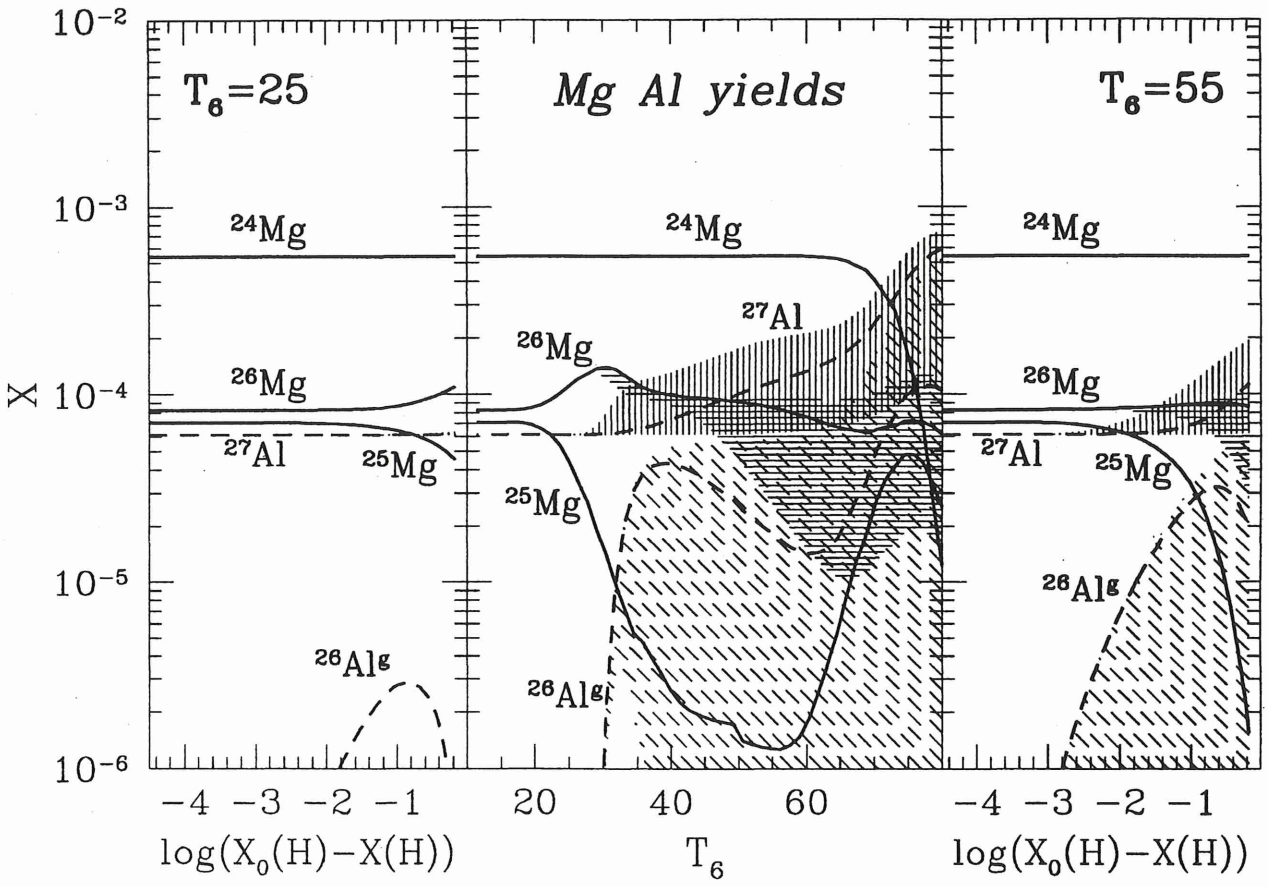

Figure 11: Same as Fig. 2, but for the nuclides involved in the MgAl chain.

remaining in the CH95 evaluation of the other ^{27}Al production mode ^{26}Mg(p,γ)^{27}Al (Fig. 10). On top of the uncertain production of ^{27}Al, the efficiency of its destruction cannot be reliably predicted either. This comes from the uncertainties remaining in the ^{27}Al(p,α)^{24}Mg and ^{27}Al(p,γ)^{28}Si rates, as displayed in Fig. 12.

The uncertainties in the ^{27}Al proton capture rates also impact on the prediction concerning the cycling character of the MgAl chain, as determined by the ratio of the ^{27}Al(p,γ)^{28}Si and ^{27}Al(p,α)^{24}Mg rates. From the data displayed in Fig. 13, and when the nuclear uncertainties are duly taken into accout, it appears that a MgAl cycle could possibly set in for $T_6 \lesssim 65$. Clearly, further work is required in order to improve our knowledge of the ^{27}Al proton capture rates, and thus to specify the extent of the leakage out of the MgAl region.

The large uncertainties in the ^{26}Al and ^{27}Al yields that relate to the destruction or production of ^{26}Al and ^{27}Al, as well as to the level of cycling of the MgAl chain, are especially unfortunate in view of the prime importance of these two nuclides in cosmochemistry and γ-ray astronomy. On the one hand, there is now ample observational evidence that ^{26}Al has decayed in situ in various meteoritic inclusions, where the $(^{26}Al^g/^{27}Al)_0$ ratio at the beginning of the condensation of the solar system solids has the "canonical" value of about $5\ 10^{-5}$ (e.g. Wasserburg 1985). There is also strong observational evidence for its decay in identified single grains of likely stellar origin, where the $^{26}Al^g/^{27}Al$ ratio can vary in the quite wide $10^{-5} \lesssim {}^{26}Al^g/^{27}Al \lesssim 1$ range (e.g. Anders and Zinner 1993, Nittler et al. 1994). On the other hand, the 1.8 MeV γ-ray emission observed in the galactic disk is attributed to the decay of about $1.5\,M_\odot$ of $^{26}Al^g$

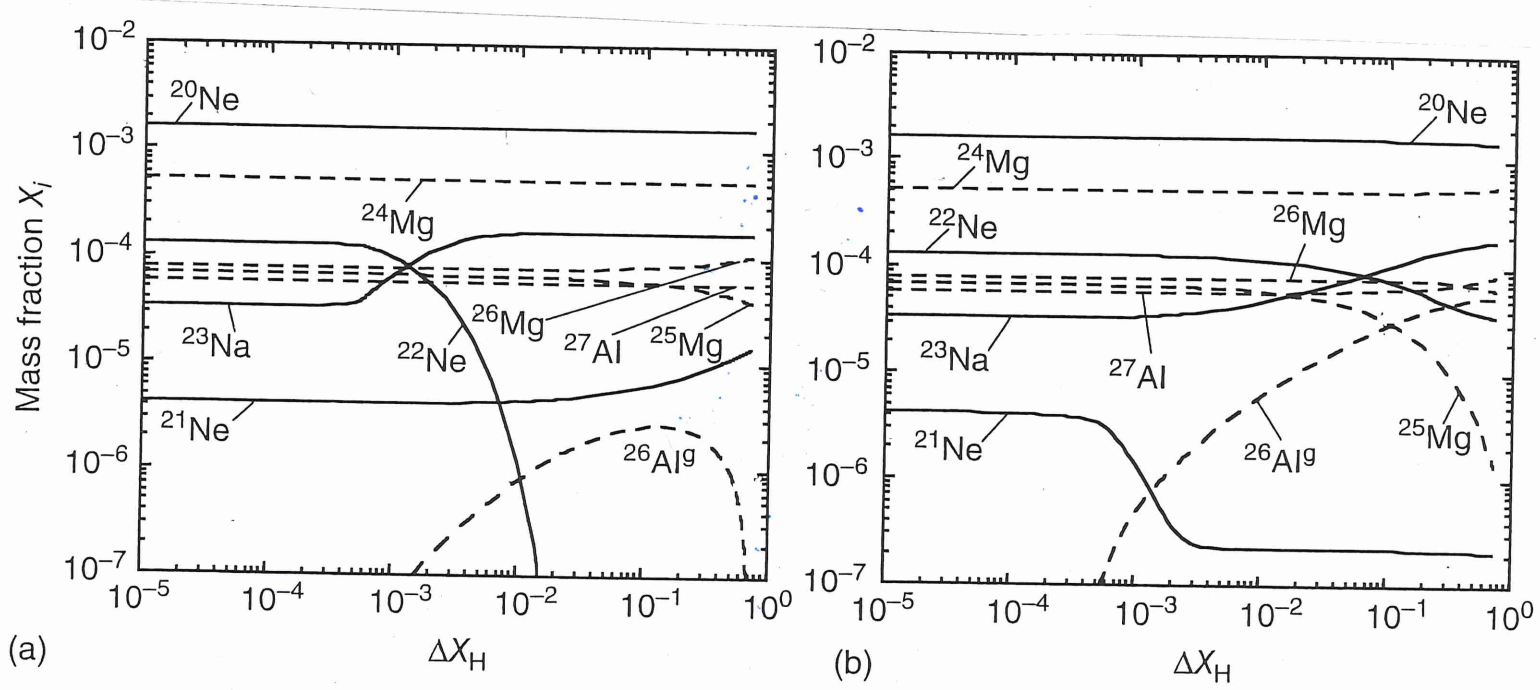

Figure 5.19 Abundance evolutions in the $A \geq 20$ mass region versus the amount of hydrogen consumed for two different constant temperatures: (a) $T = 25$ MK, and (b) $T = 55$ MK. The density ($\rho = 100$ g/cm^3) and the initial composition (solar) is the same for both cases. All curves shown are obtained by solving the reaction network numerically. The calculations are terminated when the hydrogen mass fraction falls below $X_H = 0.001$.

HELIUM BURNING

Where?

— LOW MASS

- He-core flash at tips of RGB : $M < 2.25 M_\odot$
- He-core burning or HB
- He-shell burning and thermal pulses

— HIGH MASS

- He-core burning

Many consequences for nucleosynthesis: direct and indirect

3α-process $\rightarrow {}^{12}C$

${}^{12}C(\alpha,\gamma) \rightarrow {}^{16}O$

${}^{16}O(\alpha,\gamma)\,{}^{20}Ne$

A little history!

- Need way around $A=5$ and $A=8$ gaps: $p + {}^4He$ and ${}^4He + {}^4He$ are 'forbidden'

- ${}^4He + {}^4He \rightleftharpoons {}^8Be$ { "Opik / Salpeter
  but if
  ${}^8Be + {}^4He \rightarrow {}^{12}C$

  3α-process

- Initial estimates of 3α rate were slow and $\lesssim {}^{12}C(\alpha,\gamma){}^{16}O$
  ∴ little ${}^{12}C$ survives as it is quickly converted to ${}^{16}O$
  BUT $C/O \sim 1$ IS OBSERVED

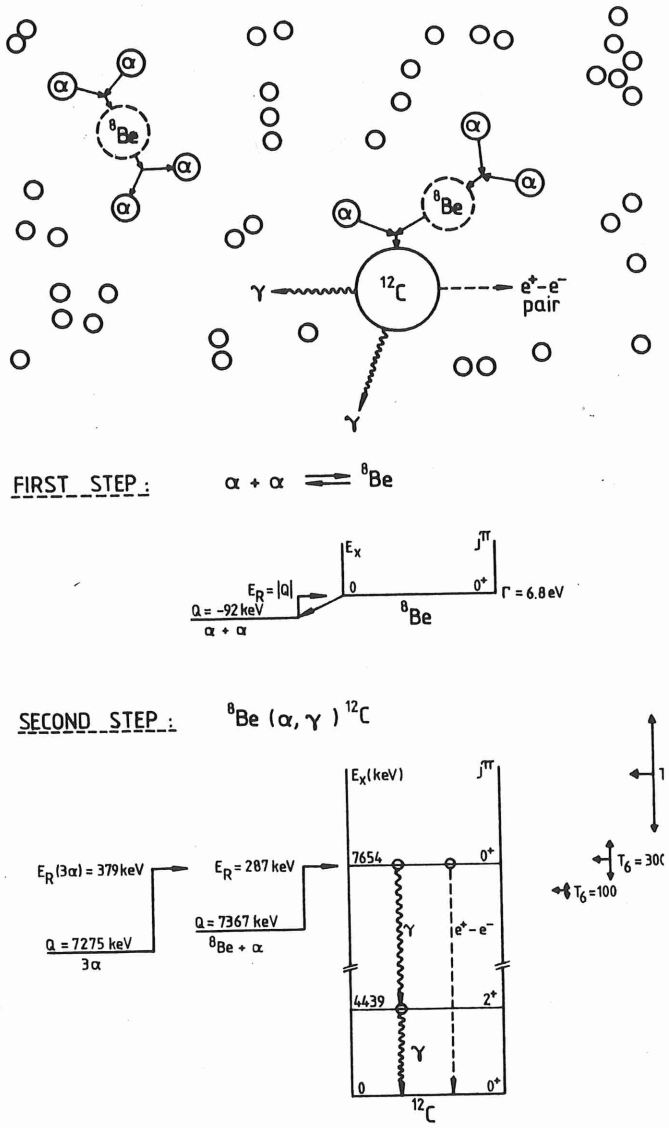

FIGURE 7.3. Schematical representation of the process by which ^{12}C can be s only ^{4}He nuclei, commonly called the triple-α process or "Salpeter-process." In this process, a small abundance of ^{8}Be nuclei is built up to equilibrium with its products. An additional α-particle is captured by the ^{8}Be nuclei, thus completing process. This capture reaction proceeds via an s-wave resonance, which is loc Gamow energy region indicated for several temperatures.

- Hoyle (1953) proposed 3α-process proceeded through a resonance with a 0^+ state in ^{12}C, a state not then known experimentally.
  Soon, found!

  For estimation of 3α rate - see Caughlan §7.1

- Recent news:

  1 – Fynbo et al. 2005, Nature, 433, 136
  Revised NACRE rate by showing that a ^{12}C level at 9.1 MeV (2^+) does not exist. (Study $^{12}C \rightarrow 3\alpha$ via β-decay for ^{12}N and ^{12}B.)

  Change of rate at low T and high T (see figure)

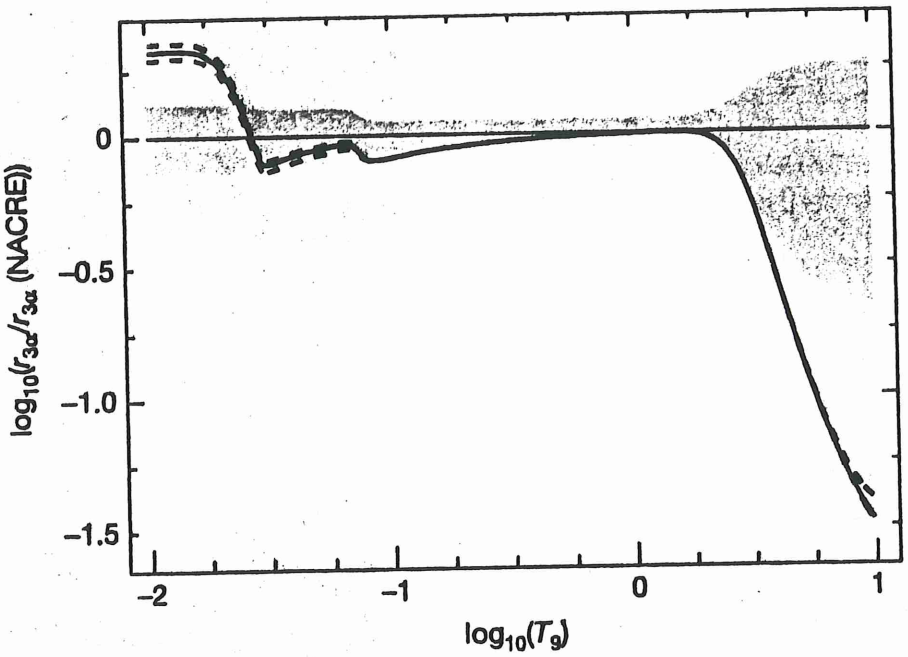

Figure 3 The triple-α reaction rate from this work, $r_{3\alpha}$, relative to the value from the current NACRE compilation[3], $r_{3\alpha}$(NACRE). T_9 is the temperature in 10^9 K. Solid line, ou rate including only the Hoyle resonance; dashed lines, our rate including the broad 0^+ resonance and its interference with the Hoyle resonance; and grey band, estimated erro band from NACRE[3] (the uncertainty in the position of their assumed 2^+ resonance is nc included). We assume that the reduced γ-decay width of the broad 0^+ resonance is equa to that of the Hoyle resonance, and the dashed lines differ only in the sign of the

2 — Ogata et al. (Prog. Theor. Phys. 122 1055, 2009)

Report on quantum calculation of non-resonant 3α process.

i.e., at energies where Hoyle state is NOT reached.

Result 10^{20} × NACRE for $T \sim 10^7$ K

NONSENSE!

Dotter & Paxton (2009, A&A 507, 1617) show new rate → He core flash at very low luminosities and no red giant branch.

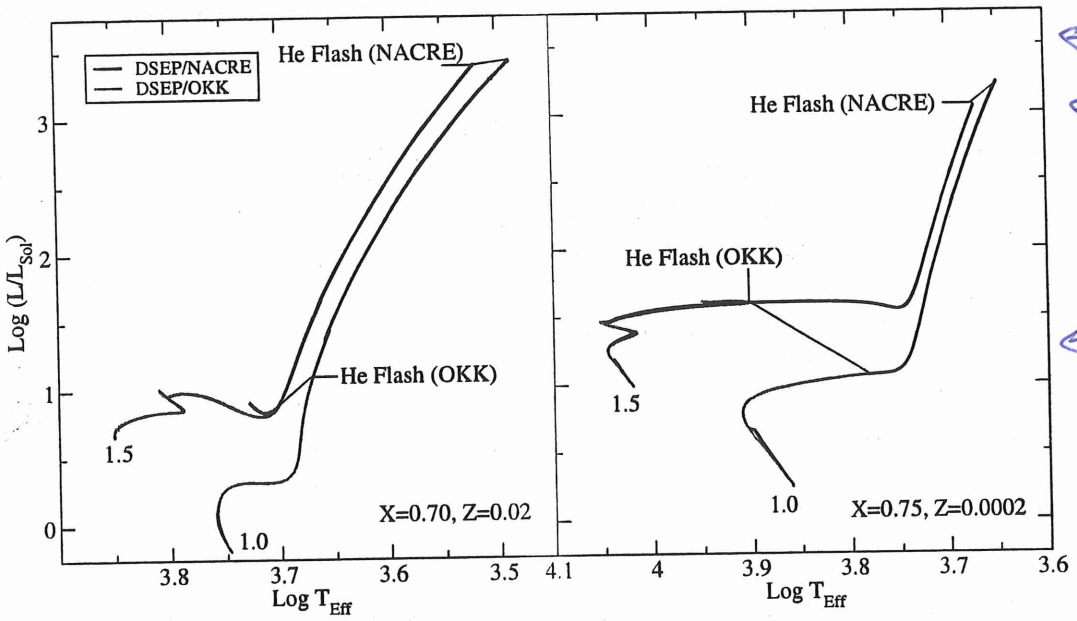

~ OBSERVED

← NO RGB!

Fig. 1. DSEP models in the H-R diagram for $X = 0.7$, $Z = 0.02$ (*left panel*) and $X = 0.75$, $Z = 0.0002$ (*right panel*). Evolutionary tracks for 1 and 1.5 $M_{\odot}$ are shown in both panels.

$^{12}C(\alpha,\gamma)^{16}O$

- Major influence on n' synthesis yet an uncertain rate for a long time — and still?

- Very small σ → measurements terminate at $E_{CM} \sim 2$ MeV but stellar rate needed at $E \sim 0.3$ MeV

  Extrapolation complicated because of two subthreshold resonances which have a small effect at σ (> 2 MeV) where an excited state resonance is a major player.

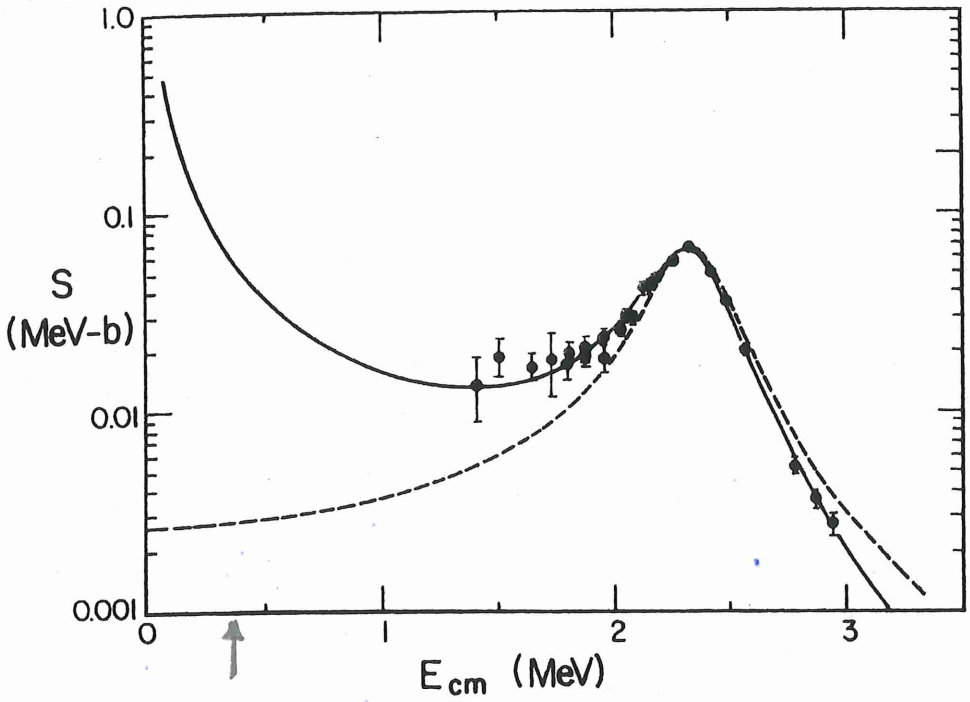

Fig. 2.12. S-factor for $^{12}C(\alpha, \gamma)^{16}O$. The dashed curve ignores the sub-threshold resonances, while the continuous curve allows for them, but the uncertainties are still significant at low energies. Koonin, Tombrello and Fox (1974). Reproduced with kind permission of Elsevier Science. Courtesy S. E. Koonin.

↑
He-core burning

[PAGEL]

Extrapolation is .....

$^{12}C(\alpha,\gamma)^{16}O$

Latest:

An et al. 2015 Phys Rev C92 045802
2015 Astr Lett 811 L5

R-matrix: no new data, but consideration of all available data.

$S(0.3\ MeV) = 162.7 \pm 7.3$ (keV b)
5%?

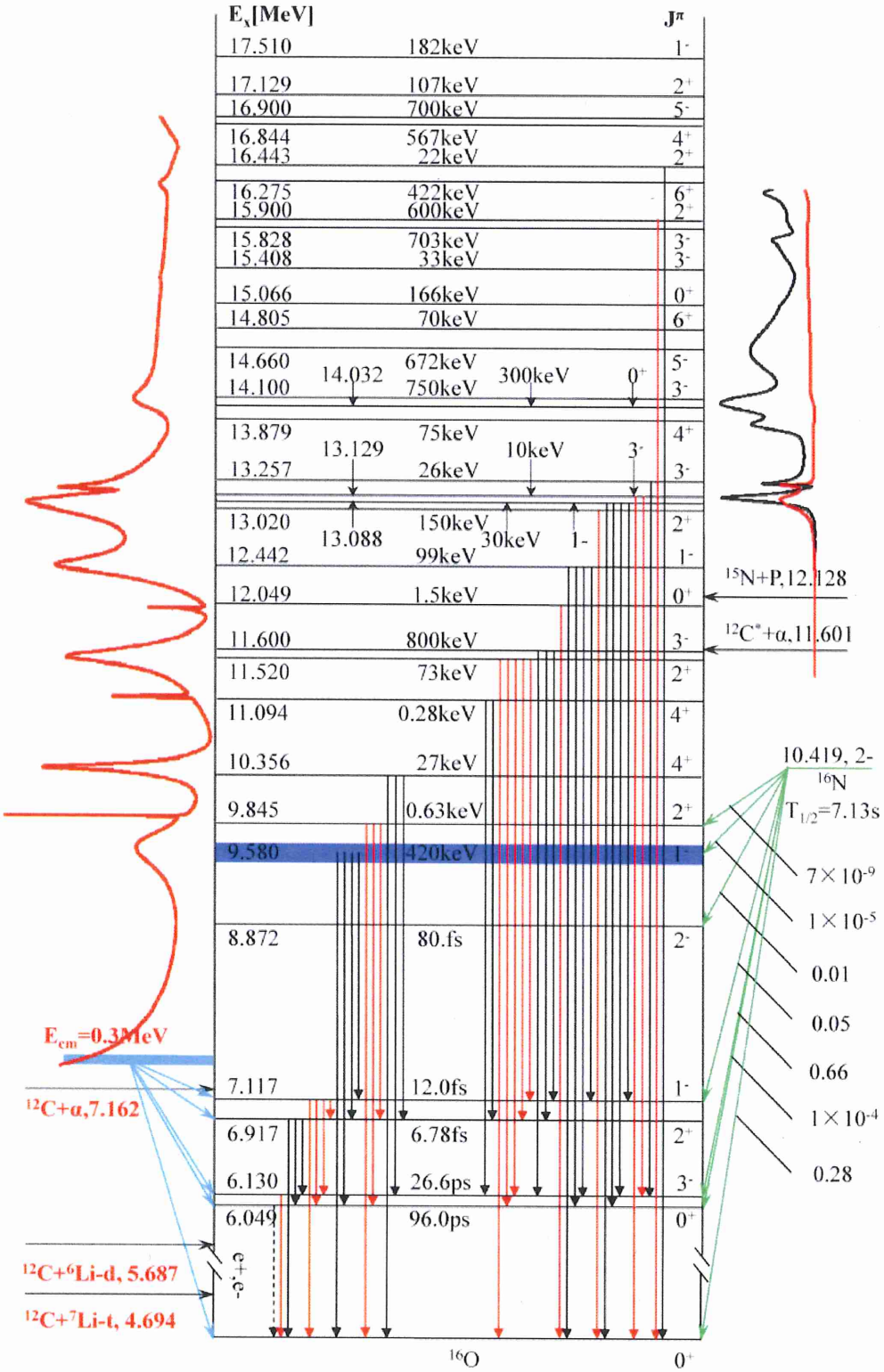

FIG. 2. (Color online) Level scheme of the ^{16}O nucleus [60]. All states relevant for the analysis are indicated.

C. Iterative fit

The fits to the data of ^{16}O system are iterated to achieve internal consistency. A file is a fixed record of the original data, which is to provide the original statistical error for the fit. Another file is a dynamic data file recording the evaluation process, whose role is to provide the actually-used data in fitting and which is updated in the iterative process. In the

$\langle \sigma v \rangle$ at He-core burning T dependson

- Low energy tail of 9.58 MeV state
- sub-threshold resonances at 7.117 and 6.917 MeV
- direct cascades to ground state

+ interference

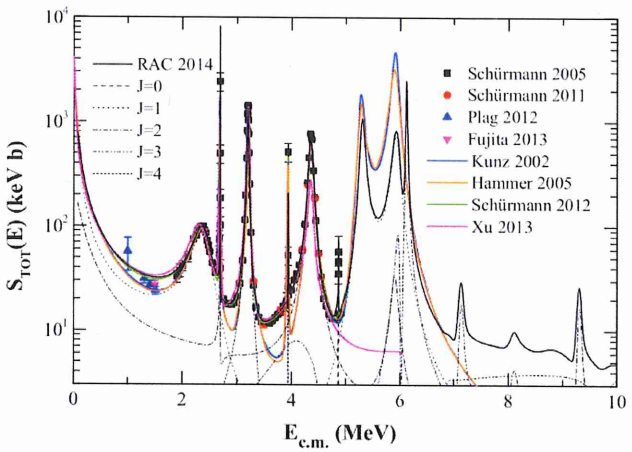

FIG. 4. (Color online) Results of the best R-matrix fit for the S_{tot} data from Schürmann 2005 [7], Schürmann 2011 [8], Plag 2012 [9], and Fujita 2013 [10], together with the decomposition into different energy-level contributions. For comparison, the results of Kunz 2002 [65], Hammer 2005 [43], Schürmann 2012 [40], and Xu 2013 [66] are also shown, respectively.

A quick survey of recent determinations for $^{12}C(\alpha,\gamma)^{16}O$ rate

1. Many papers including those on n' synthesis by massive stars bemoan the lack of an accurate rate at astrophysical energies

"The key uncertain reaction rate affecting the structure of and nucleosynthesis in massive stars remains $^{12}C(\alpha,\gamma)^{16}O$ despite over 30 years of painstaking laboratory investigation." Woosley & Heger (2007, Physics Reports, 442 269)

2. For many stellar studies $S(300)$ is needed near 300 keV, that is $S(300)$ sought

Kunz et al. (2002 ApJ 567 643) Table 1 list $S(300)$ from 1974 to 2001 for S_{E1}, S_{E2}, S_{tot}.

Their recommendation $S(300) = 165 \pm 50$ keV-b

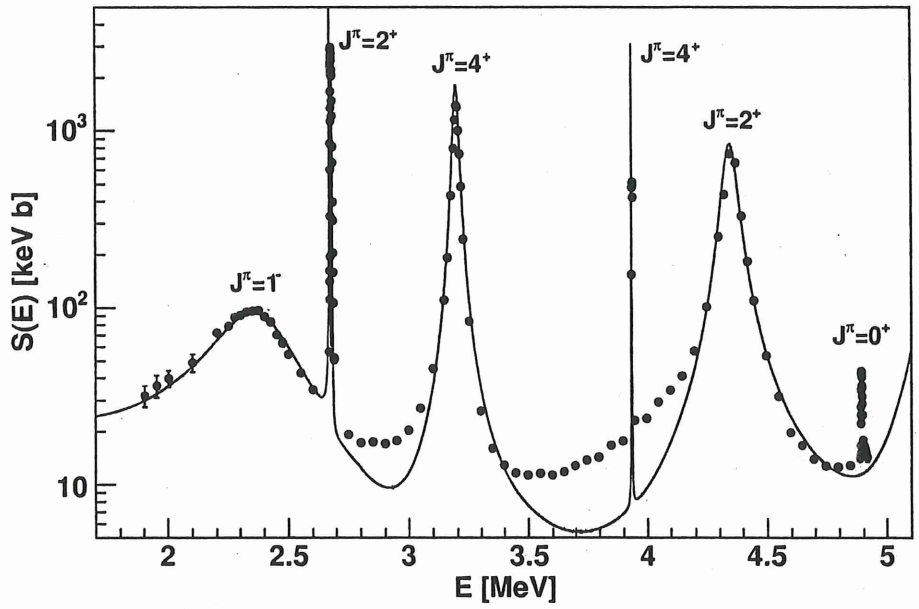

Fig. 3. Total $S(E)$ factor of the reaction $^{12}C(\alpha,\gamma)^{16}O$. Data near the narrow resonances at $E = 2.68, 3.9$, and 4.9 M target yields. The solid line represents the sum of the different amplitudes extracted from a recent R-matrix ca Error bars shown are statistical only.

Schürmann et al. (2005)

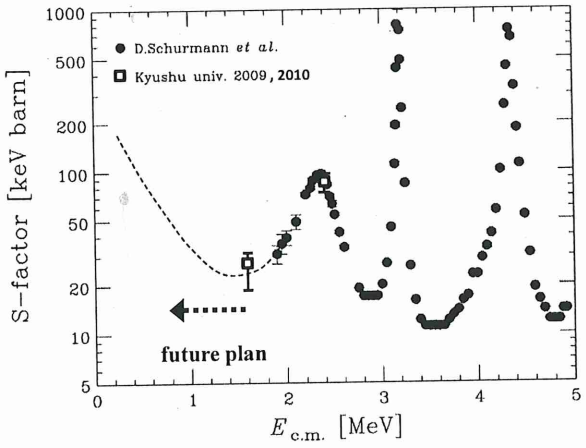

Figure 5: Preliminary results for the astrophysical S-factor as a function of the center-of-mass energy. The closed circles between E_{cm} = 5.0 to 1.9 MeV represent data obtained by Ruhr University [4], while the two open squares represent data obtained by our experiments in 2009 and 2010.

3. First DIRECT measurement of total σ for $^{12}C(\alpha,\gamma)^{16}O$

Schürmann etal. 2005 Eur Phys. J. A 26 301

(also Fujita etal. PoS(NIC X) 18, 2011)

No extrapolation to 300 keV described.

^{12}C beam on ^4He target → ^{16}O recoils

4. Measurements of the angular distribution of capture γ-rays

Assunção etal. 2006, Phys. Rev. C 73 055801

Hammer etal. 2005, Nucl. Phys. A 758, 363

Measurements ⇒ 1.3 MeV (c-max)

$S_{tot}(300) = 162 \pm 39$ keV-b

5. E1 to 450 keV, $^{16}N \rightarrow d + ^{12}C$

Tang etal. 2010 Phys Rev C 045809

$S_{E1}(300) = 86 \pm 22$ keV b

6. ASTROPHYSICAL

(Boyd Fig 6.5, Pagel Fig 5.11)

Woosley & Heger 2007, Phys. Rep. 442, 269

Best fit 1.2 × Buchmann or

S(300) = 183 keV-b

BUT correction, ------

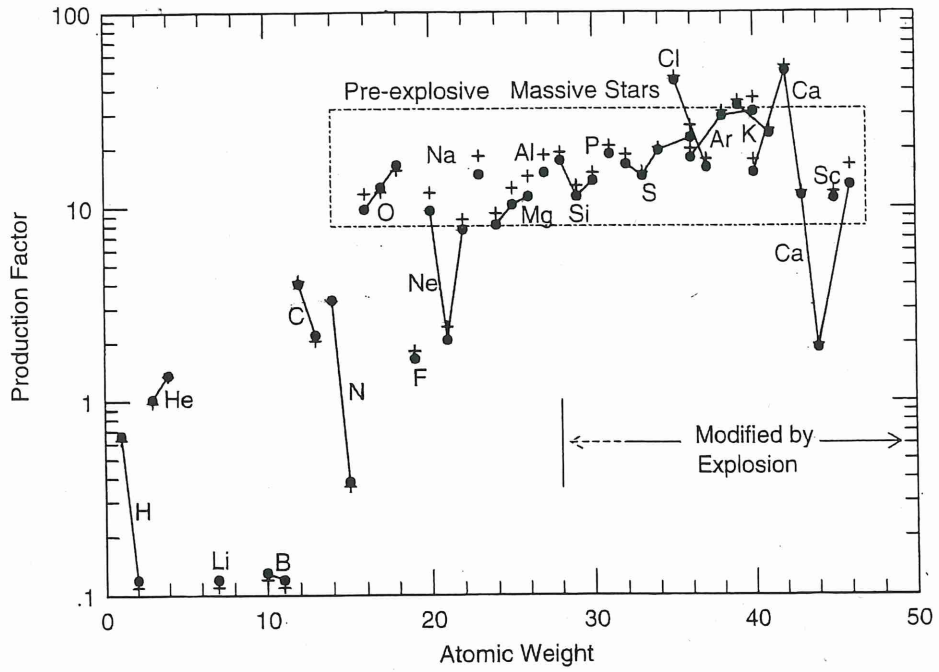

Fig. 5.11. Amounts, in units of relative Solar-System abundances, of nuclear species resulting from hydrostatic evolution of an average pre-supernova. Filled circles represent an initial mass function with slope -2.3 and plus signs one with slope -1.5. The dashed box encloses 28 species co-produced within a factor of 2 of solar values, assuming a $^{12}C(\alpha, \gamma)^{16}O$ rate 1.7 $\times$ that given by Caughlan and Fowler (1988). Reprinted from Weaver and Woosley (1993). Reproduced with kind permission of Elsevier Science. Courtesy Tom Weaver.

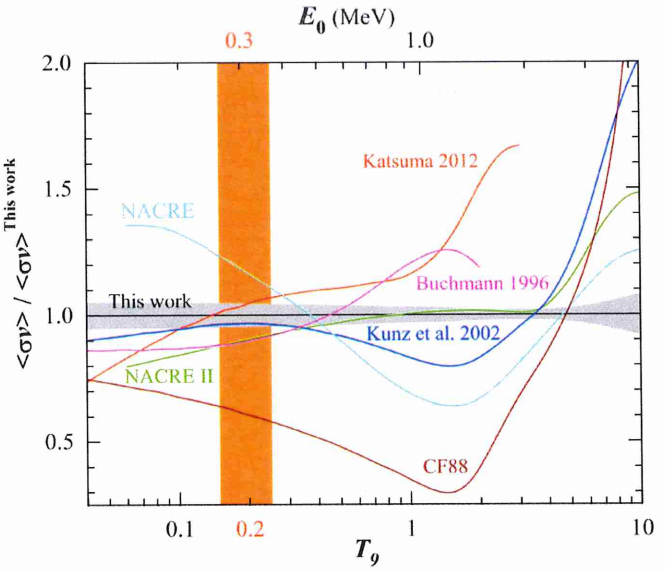

Figure 4. Comparisons of the astrophysical reaction rate of $^{12}C(\alpha, \gamma)^{16}O$ (including CF88) normalized to our new recommended rate.

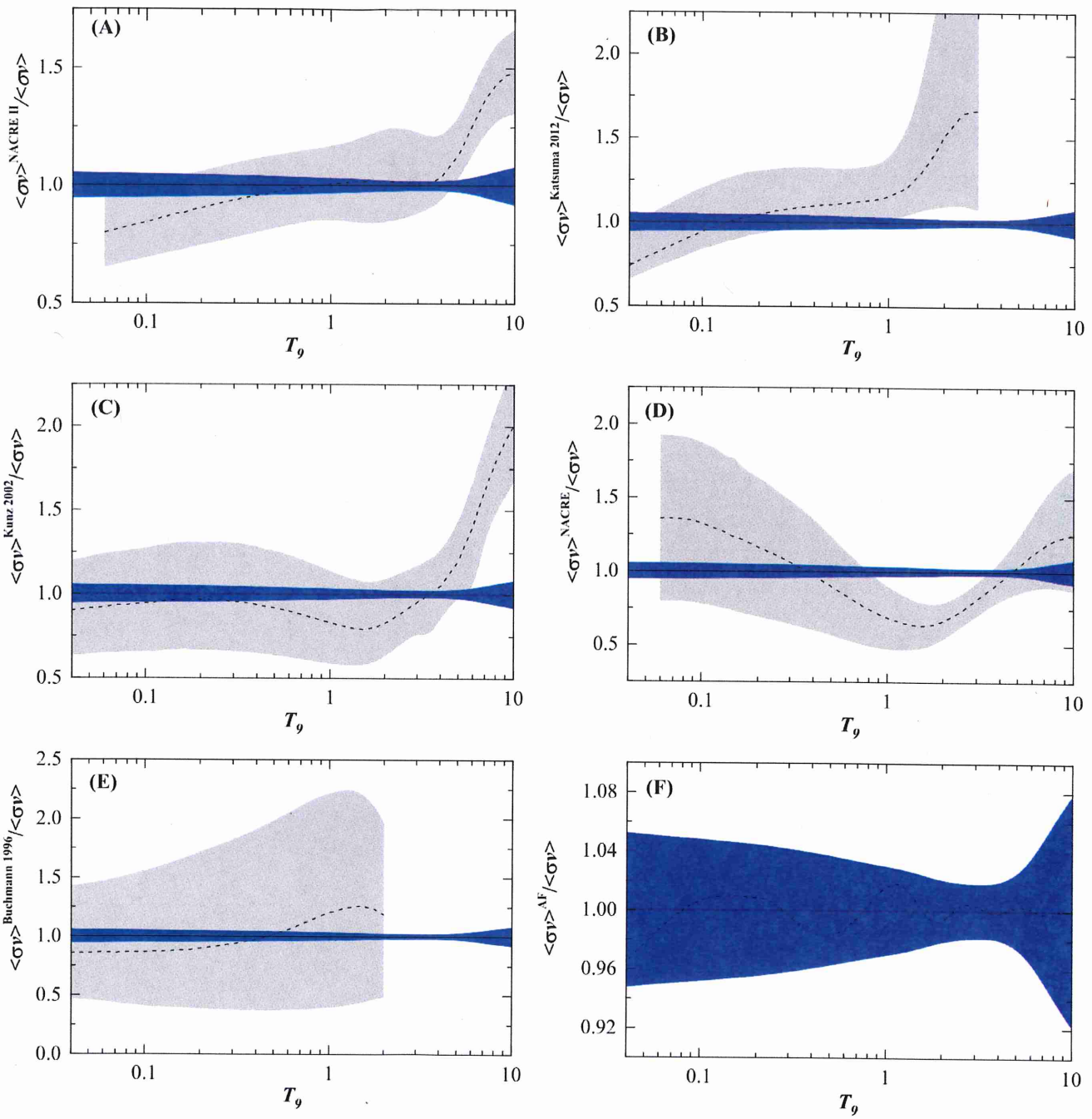

Figure 3. Comparisons (ratio) of $^{12}C(\alpha, \gamma)^{16}O$ reaction rates from the compilations of (A) NACRE II, (B) Katsuma (2012), (C) Kunz et al. (2002), (D) NACRE, and (E) Buchmann (1996) with our new recommended rate. The accuracy of the analytic formula according to Equation (2) is shown in Figure 3(F).

EFFECTS of $^{12}C(\alpha,\gamma)^{16}O$ UNCERTAINTIES

General: Ratio of $^{12}C(\alpha,\gamma)^{16}O$/3$\alpha$ rates

→ Massive star evolution in and beyond He burning up to Si

- pre-SN progenitors ($>9M_\odot$) structure
- explosive nucleosynthesis
- remnant mass

Since 3α-rate is well determined, the $^{12}C(\alpha,\gamma)^{16}O$ uncertainties are dominant

→ Affects too in AGB evolution and their remnants

See, for example,
Tur et al. 2007, ApJ 671, 821 and references therein.

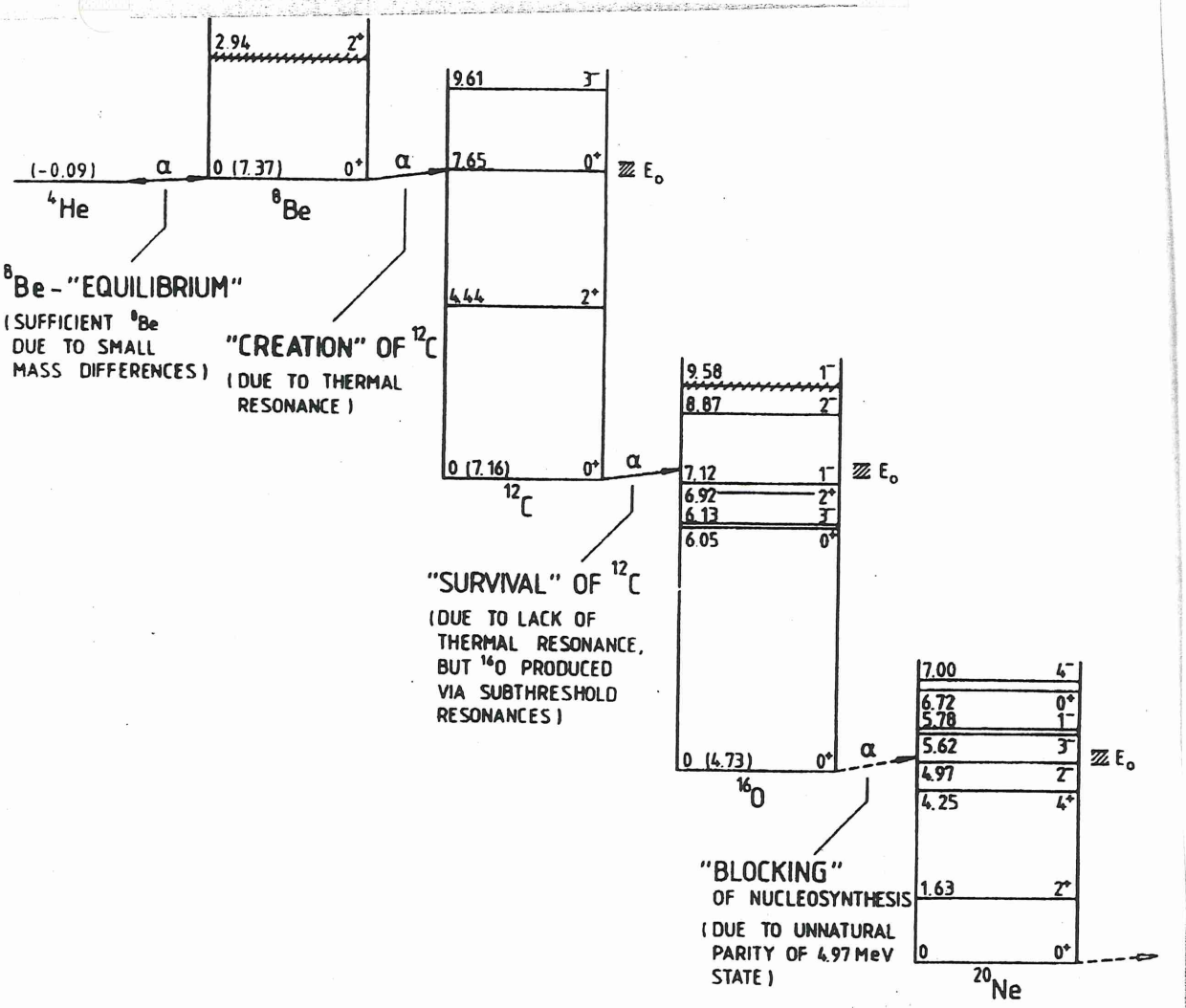

Fig. 5.8. Nuclear energy levels involved in the 3α reaction. After Rolfs and Rodney (1988). Copyright by the University of Chicago. Courtesy Claus Rolfs.

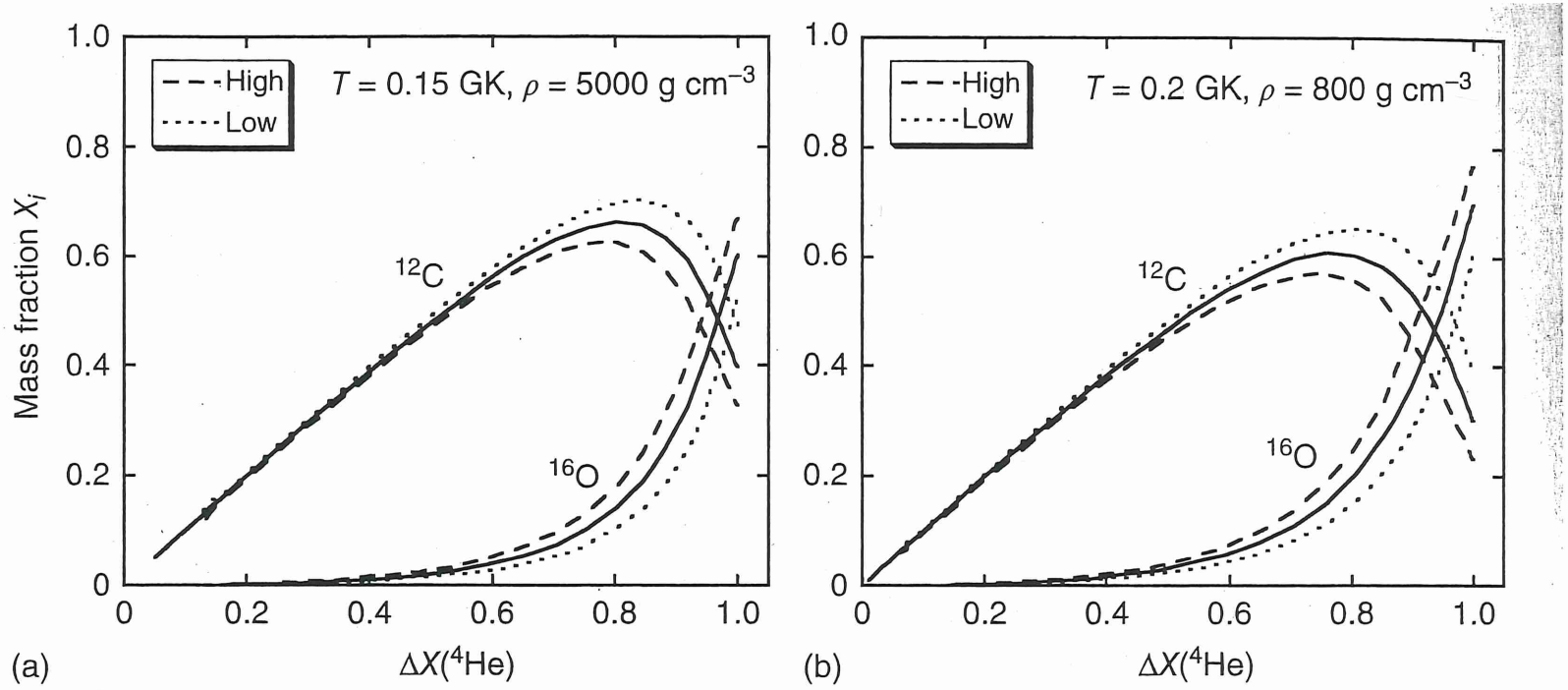

Figure 5.23 Evolution of ^{12}C and ^{16}O versus the amount of helium consumed during hydrostatic helium burning for constant temperatures and densities of (a) $T = 0.15$ GK and $\rho = 5000$ g/cm^3, and (b) $T = 0.2$ GK and $\rho = 800$ g/cm^3. The results are obtained by solving the reaction network numerically, assuming a pure ^{4}He gas at the beginning of helium burning. The calculation is terminated when the helium mass fraction falls below $X_{^4\text{He}} = 0.001$. The solid lines are obtained by adopting recommended $^{12}C(\alpha,\gamma)^{16}O$ reaction rates, while the dotted and dashed lines result from using the lower and upper limit of the $^{12}C(\alpha,\gamma)^{16}O$ reaction rates, respectively.

REACTIONS ACCOMPANYING $^{12}C(\alpha,\gamma)^{16}O$

- $^{16}O(\alpha,\gamma)^{20}Ne$ is "blocked" in He-core burning
  - Coulomb barrier again
  - few and unsuitable resonances at T(He burning)

  (Caughlan p407)

- $^{14}N \rightarrow {}^{22}Ne$

  $^{14}N(\alpha,\gamma)^{18}F(\beta^+\nu_e)^{18}O(\alpha,\gamma)^{22}Ne$

  - competition with $^{18}O(\alpha,n)^{21}Ne$
  - rates $\simeq$ at $T_9 \sim 0.6$
    - $T_9 < 0.6$ $(\alpha,\gamma) > (\alpha,n)$
    - > 0.6 $(\alpha,n) > (\alpha,\gamma)$

As long as $T_9 < 0.6$, 'ALL' (CNO)$_{\text{initial}} \rightarrow {}^{14}N$ as 'all' $^{14}N \rightarrow {}^{22}Ne$

Hence,

i) ^{22}Ne with $Z=10$ but $N=12$ carries a neutron excess. This is a quantity NOT changed in explosive nucleosynthesis (β-decays are slow.)

ii) ^{22}Ne is a potential n-source in massive stars and in AGB He-shells (see s-process discussions)

: $^{22}Ne(\alpha,n)^{25}Mg$ in competition with $^{22}Ne(\alpha,\gamma)^{26}Mg$

- again, 'uncertain' rates!

iii) $^{14}N \rightarrow {}^{22}Ne$ incomplete during He-shell burning $\rightarrow$ ^{18}O synthesis

iv) Also, $^{18}O(p,\alpha)^{15}N(\alpha,\gamma)^{19}F$ with $^{14}N(\alpha,p)^{17}O$ in He-shell burning

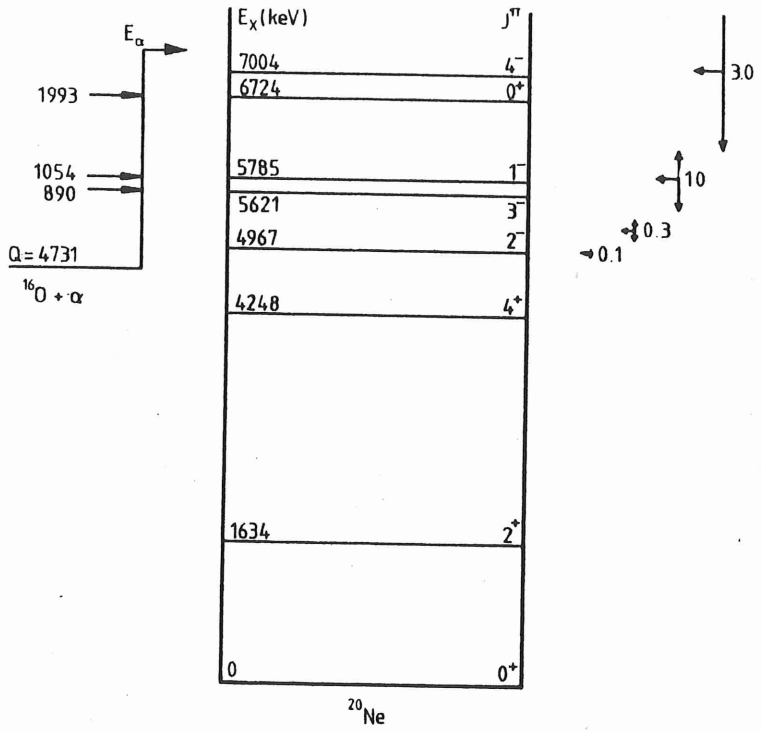

FIGURE 7.12. Energy levels of the ^{20}Ne nucleus in the region of the α-particle threshold (Ajz83). Shown also are the most effective energy regions for temperatures from $T_9 = 0.1$ to $T_9 = 3.0$. Note that the $J^\pi = 2^-$ and $J^\pi = 4^-$ levels do not produce resonances in $^{16}O(\alpha, \gamma)^{20}Ne$, because of their unnatural parity.

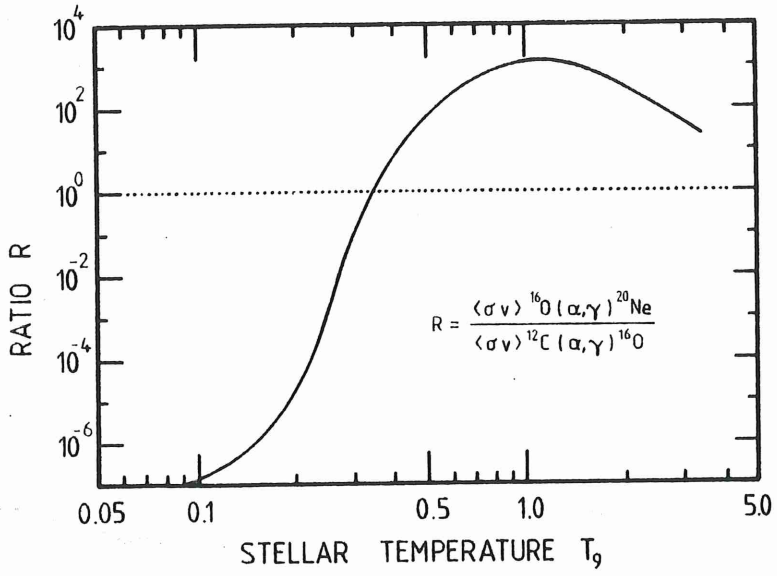

FIGURE 7.13. The ratio of the stellar reaction rates for $^{16}O(\alpha, \gamma)^{20}Ne$ and $^{12}C(\alpha, \gamma)^{16}O$ (Fow75) is shown as a function of temperature. Note that this ratio is very small at helium-burning temperatures of $T_9 = 0.1$–0.2, thus essentially blocking the nucleosynthesis beyond ^{16}O.

Table 11.2
Important Reactions in He-Burning

(a) energy generation

$$^{4}He(2\alpha,\gamma)\ ^{12}C(\alpha,\gamma)\ ^{16}O(\alpha,\gamma)\ ^{20}Ne$$

(b) neutron source

$$^{14}N(\alpha,\gamma)\ ^{18}F(\beta^{+})^{18}O(\alpha,\gamma)\ ^{22}Ne\ (\alpha,\gamma)\ ^{26}Mg$$
$$^{14}N(\alpha,\gamma)\ ^{18}F(\beta^{+})^{18}O(\alpha,\gamma)\ ^{22}Ne\ (\alpha,n)\ ^{25}Mg$$

(c) high temperature burning with effective $^{22}Ne(\alpha,n)$

$$^{22}Ne(n,\gamma)\ ^{23}Ne(\beta^{-})\ ^{23}Na(n,\gamma)\ ^{24}Na(\beta^{-})\ ^{24}Mg$$
$$^{20}Ne(n,\gamma)\ ^{21}Ne(\alpha,n)\ ^{24}Mg$$
$$^{24}Mg(n,\gamma)\ ^{25}Mg(n,\gamma)\ ^{26}Mg(n,\gamma)\ ^{27}Mg(\beta^{-})\ ^{27}A$$
$$^{27}Al(n,\gamma)\ ^{28}Al(\beta^{-})\ ^{28}Si(n,\gamma)\ ^{29}Si\ +\ \text{further s-}$$